

Photostable single-photon emission from self-assembled nanocrystals of polycyclic aromatic hydrocarbons

Sofia Pazzagli,^{*,†,‡} Pietro Lombardi,^{‡,¶} Daniele Martella,[¶] Maja Colautti,[¶] Bruno Tiribilli,[§] Francesco Saverio Cataliotti,^{†,‡,¶,||} and Costanza Toninelli^{*,‡,¶,||}

[†]*Dipartimento di Fisica ed Astronomia, Università di Firenze, Via Sansone 1, I-50019 Sesto F.no, Firenze, Italy*

[‡]*CNR-INO, Istituto Nazionale di Ottica, Via Carrara 1, 50019 Sesto F.no, Firenze, Italy*

[¶]*LENS and Università di Firenze, Via Carrara 1, 50019 Sesto F.no, Firenze, Italy*

[§]*CNR-ISC Istituto dei Sistemi Complessi, via Madonna del Piano 10, I-50019 Sesto F.no, Firenze, Italy*

^{||}*QSTAR, Largo Fermi 2, I-50125 Firenze, Italy*

E-mail: sofia.pazzagli@unifi.it; toninelli@lens.unifi.it

Abstract

Quantum technologies could largely benefit from the control of quantum emitters in sub-micrometric size crystals. These are naturally prone to the integration in hybrid devices, including heterostructures and complex photonic devices. Currently available quantum emitters sculpted in nanocrystals suffer from spectral instability, preventing their use as single photon sources *e.g.*, for most quantum optics operations. In this work we report on unprecedented performances of single-photon emission from organic nanocrystals (average size of hundreds nm), made of anthracene (Ac) and doped with

dibenzoterrylene (DBT) molecules. The source has hours-long photostability with respect to frequency and intensity, both at room and at cryogenic temperature. When cooled down to 3 K, the 00-zero phonon line shows linewidth values (50 MHz) close to the lifetime-limit. Such optical properties in a nanocrystalline environment make the proposed organic nanocrystals a unique single-photon source for integrated photonic quantum technologies.

The ubiquitous deployment of nanocrystals (NCs) in photonics stems from the impressive tunability of their physical and chemical properties, combined with the nano-positioning opportunities offered by support-free colloids and from the possibility of mass-production at low costs.¹ These features have also promoted NCs as efficient biological markers for imaging,^{2,3} color filters in liquid crystal displays,⁴ as well as functionalizing elements in light emitting and light harvesting devices.⁵ On the other hand, advanced nanophotonic applications are emerging based on the generation, manipulation and detection of single photons.^{6,7} Indeed, leveraging single-photon statistics and quantum coherence for sub-diffraction imaging,⁸ quantum cryptography,⁹ simulation,¹⁰ enhanced precision measurements and information processing¹¹ have become roadmap targets for the next 10-20 years.¹² Single-photon sources based on quantum emitters hold promise for these applications because of their on-demand operation.¹³⁻¹⁷ However, despite great efforts in the last years to attain controllable sources by coupling solid-state emitters to nanophotonic structures, each platform privileges either the freedom in the device design¹⁸⁻²³ or the quality of single-photon emission.^{24,25} Deterministic positioning and control of quantum emitters remains elusive for epitaxial quantum dots,²⁶⁻²⁹ color centers in bulk diamond^{30,31} and organic molecules in crystalline matrices.³²⁻³⁵ On the other hand, versatile approaches based on today-available NCs present important shortcomings with respect to single-photon applications. Photoinduced charge rearrangements in the passivation layer and in the environment of inorganic semiconductor quantum-dot NCs^{36,37} lead to spectral instability of the exciton line,³⁸ hindering basic quantum optics operations with the emitted photons. Moreover, intermittence in the photoluminescence,³⁹

named blinking, seriously affects the average fluorescence quantum yield and hence the photon state purity. Although important results have been obtained by improving synthesis protocols⁴⁰ or introducing perovskite materials,^{41,42} the emitter photostability in time or frequency is still below expectations. Notably, similar issues characterize the emission of color centres in nanodiamonds, including those which possess superb optical properties in bulk such as the widely studied negatively charged silicon vacancy,^{16,43} or chromium-related defects.⁴⁴ Hence, despite the wealth of materials and protocols, there still are fundamental limitations for the use of NCs in single-photon applications.

We here propose and report on self-assembled and support-free organic NCs (hundreds nm in size) of anthracene doped with single fluorescent dibenzoterrylene molecules (DBT:Ac). We demonstrate that the remarkable features of the bulk system,⁴⁵⁻⁴⁷ belonging to the family of Polycyclic Aromatic Hydrocarbons (PAH), are preserved in a nanocrystalline environment. In particular, DBT:Ac NCs exhibit bright and photostable single-photon emission at room temperature that is spectrally stable and almost lifetime-limited (50 MHz) at cryogenic temperatures. The combination of such properties is unique and opens the way to the use of organic NCs for quantum technologies and for single-photon applications in general.

Results and discussion

We adapted a simple, cost-effective and well-established reprecipitation method⁴⁸⁻⁵¹ to grow Ac NCs doped with controlled concentration of DBT molecules (for details see the Experimental Section). In this procedure, a dilute solution of the compounds prepared with a water-soluble solvent (acetone, in our case) is injected into sonicating water where it divides into many droplets. The solvent gradually dissolves and correspondingly the concentration in the micro-droplets becomes super-saturated until the compounds, which instead are not water-soluble, are reprecipitated in the form of NCs. The size and shape of the resulting NCs can ideally be controlled by varying the thermodynamic conditions.⁵²

For morphological and optical characterization, a drop of the suspension of NCs in water is deposited on a coverglass substrate and dried in desiccator. Typical scanning electron microscopy (SEM) and atomic force microscopy (AFM) images are displayed in Figures 1a and 1b, respectively. For some NCs it is possible to identify peculiar features of crystalline Ac - such as the hexagonal-like morphology - while others exhibit a round-like shape, possibly due to a few nm acetone-rich solvent cage. By analysing the AFM images of 92 NCs (Figure 1d), we deduce an average equivalent diameter of (113 ± 64) nm and an average thickness of (65 ± 13) nm, compatible with a platelet-like shape. Such values and shape are particularly promising for the coupling to evanescent fields in proximity to surfaces.³⁵ The crystalline

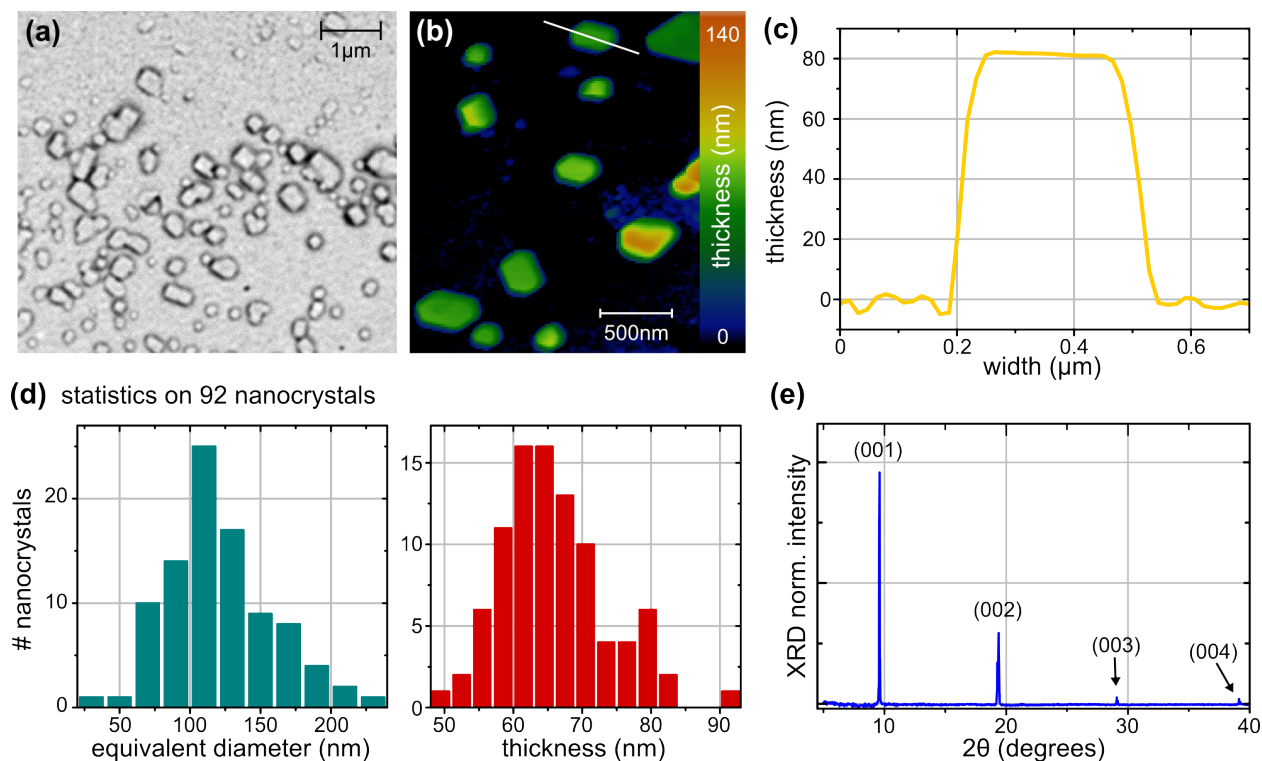


Figure 1: **Morphology of DBT:Ac NCs grown via reprecipitation:** Typical SEM (a) and AFM topography (b) images. (c) Cross section showing the NC thickness profile along the white line in panel (b). (d) Statistical analysis on AFM images yielding a NC equivalent diameter and standard deviation of (113 ± 64) nm and an average thickness of (65 ± 13) nm. (e) Normalized XRD pattern in which only the peaks from the (001) plane and higher order reflections are well resolved, due to the NCs' platelet-like morphology (with c-axis perpendicular to the substrate).

nature suggested by the clear-cut edges and flat surfaces (see Figure 1c) is verified by X-ray diffraction (XRD) measurements. The XRD pattern shown in Figure 1e exhibits a strong diffracted peak at 9.17° - that corresponds to the (001) plane - and other equivalent periodic peaks corresponding to the (002), (003), and (004) planes, matching the crystallographic data for an anthracene monoclinic system.⁵³ This also reveals that the Ac NCs, once deposited on the substrate, are mainly iso-oriented with the c-axis perpendicular to the substrate. Let us note that the transition dipole moment of a DBT molecule in the main insertion site of an Ac crystals is mostly oriented along the b-axis,⁵⁴ and thus results parallel to the substrate.

The sub-micrometric size of the crystalline matrix may compromise the optical properties of DBT molecules embedded therein, due to strain within the crystal and imperfections at the interfaces. Indeed, besides the case of quantum dots, it was reported for other nanocrystalline systems that such effects determine fluorescence instability and linewidth broadening.^{43,55} We thus perform single molecules microscopy and spectroscopy on DBT:Ac NCs with a home-built epifluorescence scanning confocal microscope - described in details in the Experimental Section - that allows for both room and cryogenic temperature investigation.

At room temperature (RT), the sample is illuminated with a 767 nm continuous wave (CW) diode laser to pump DBT molecules into the vibrational band of the first singlet electronic excited state (see the simplified Jablonski diagram in Figure 2a). After a fast (ps-timescale) non radiative relaxation process to the lowest level of the vibrational manifold, molecules decay to the electronic ground state (singlet). The resulting red-shifted fluorescence light around 785 nm is detected with an electron multiplied charge couple device (EMCCD). Typical white light and wide-field fluorescence images are compared in Figure 2b, showing that more than 90% of the Ac NCs are successfully doped with DBT. To prove that the detected fluorescence stems from individual DBT molecules, single isolated crystals are illuminated in confocal mode with an excitation intensity of 15 kW cm^{-2} (well below saturation) and the correlation between photon arrival times is measured with the Hanbury Brown-Twiss (HBT) setup (see the Experimental Section). Figure 2c shows the histogram of

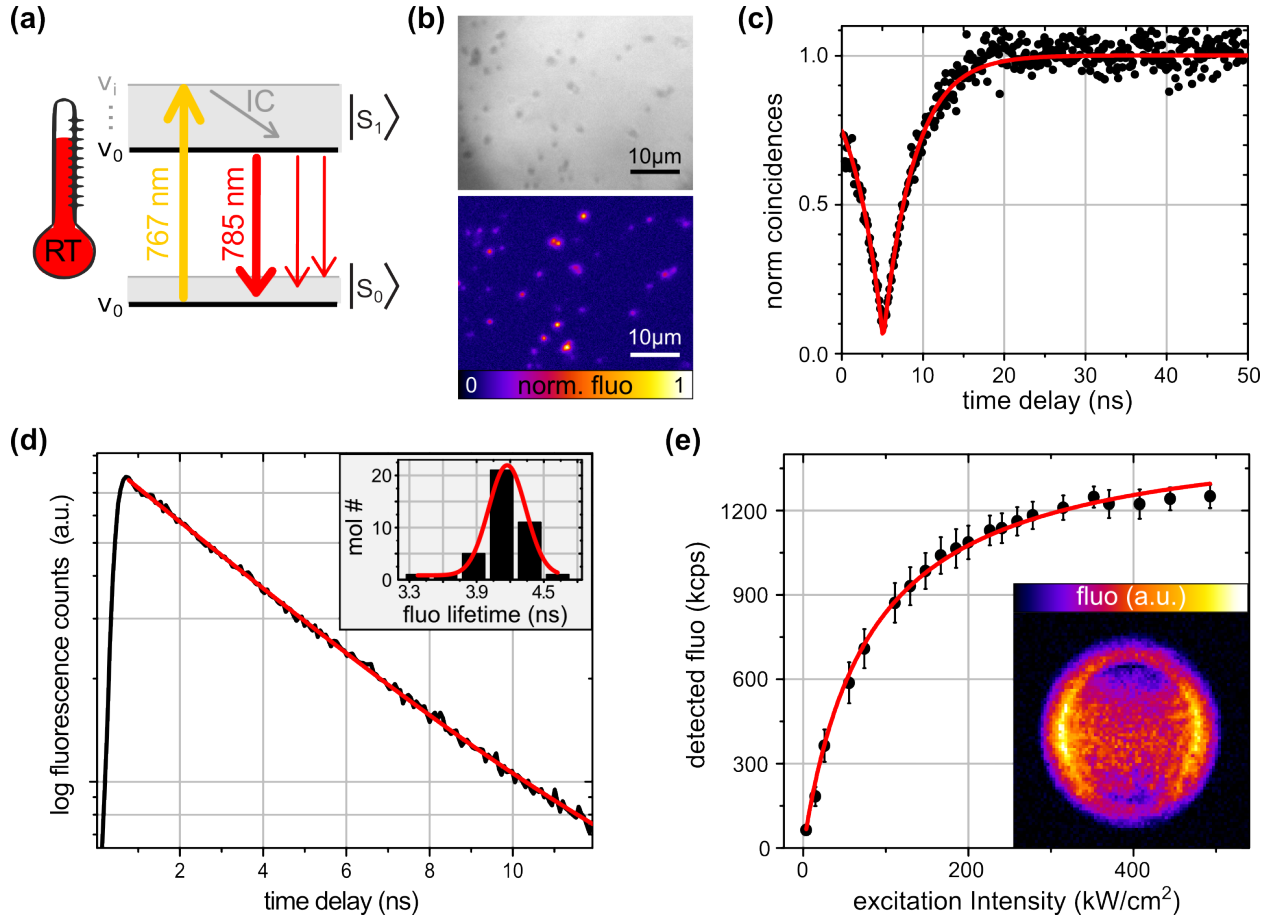


Figure 2: **Photophysics of the NCs at RT:**(a) Off-resonant pumping scheme employed for single molecule microscopy at RT. (b) Comparison between white light and fluorescence wide-field EMCCD images of the same region demonstrating that about 90% of the Ac NCs are successfully doped with DBT. (c) Measured photon anti-bunching ($g^2(0) = 0.05$ from the fit, red solid line) from the emission of a single NC without any background correction (black dots). (d) Time-resolved measurement of the fluorescence decay from a single DBT:Ac NC (black line). A single exponential fit (red line) yields an excited state lifetime of (4.2 ± 0.1) ns, as a free fitting parameter with the relative standard error. The inset shows the distribution of the excited-state lifetime collected from 40 NCs. The red curve is a Gaussian fit centered at 4.2 ns with FWHM = 0.4 ns. (e) Saturation measurement performed on a single DBT:Ac NC (black dots). The fitted red curve yields a saturation intensity of $I_s = (80 \pm 6)$ kW cm $^{-2}$ and a maximum detected count rate $R_\infty = (1.50 \pm 0.02)$ Mcps. In the inset, a typical BFP image of a single NC.

the observed coincidences from a single NC, featuring a strong antibunching dip. The experimental data is fitted at short time delays τ with the function $g^2(\tau) = 1 - b \cdot \exp(-|\tau|/\Delta t)$, where Δt accounts for the excitation and spontaneous emission rates⁴⁷ and b , the dip depth, is found to be $(95 \pm 1)\%$. Among 40 analyzed NCs, 73% of them displays an antibunching

dip larger than 50%, demonstrating that the proposed recipe is reliable to grow individual Ac NCs in 2/3 of cases doped with single DBT molecules. The purity of this system, *i.e.* the second-order correlation function at zero time delay $g^2(0)$, can be as low as 0.05 ± 0.01 without any background correction.

To gain further information on the emitter properties, we study the relaxation dynamics by means of time-correlated single-photon counting (TCSPC) measurements, collecting photons emitted after Ti:Sa-pulsed excitation (average intensity equal to 20 kW cm^{-2}) with a single-photon avalanche diode (SPAD). Figure 2d shows a typical measured fluorescence decay curve from which the lifetime τ_f of the excited state can be derived via a single exponential fit in the presence of a constant background. The fit (red curve) yields an excited state lifetime of $(4.2 \pm 0.1)\text{ns}$. Repeating the measurement on 40 NCs we obtain the distribution for the excited-state lifetime shown in the inset of Figure 2d, which can be fitted with a Gaussian centered at 4.2 ns with full width at half maximum (FWHM) of 0.4 ns, in agreement with previous studies on the bulk system.^{45,56,57}

The brightness of the NC-based single-photon source is quantified by studying the saturation behavior of the system, non-resonantly pumped with the 767 nm-CW laser. Measurements are performed at different excitation intensities, scanning the sample under the confocal laser spot in the small region where the NC is located and detecting the red-shifted fluorescence with a single SPAD. From the obtained fluorescence maps the mean value within an area around the brightest pixel is extracted and corrected for the background counts, which is the mean value within an area out of the NC and is linear with the laser power. Data are plotted as a function of the laser intensity I (black dots in Figure 2e) and fitted with the function describing the saturation of the photon detection rate $R(I)$:⁵⁸

$$R(I) = R_\infty \frac{I}{I + I_s} \quad (1)$$

with I_s the saturation intensity and R_∞ the maximum detected count rate. For the molecule

reported in Figure 2e the fit-procedure yields as free fitting parameters with the relative standard errors $I_s = (80 \pm 6) \text{ kW cm}^{-2}$ and a maximum detected count rate $R_\infty = (1.50 \pm 0.02) \text{ Mcps}$. These can be considered as typical values. Accounting for the quantum efficiency of the SPAD, $\eta_{det} = 50\%$, the measured R_∞ corresponds to a collected photon rate of 3 MHz at the detector. Moreover, comparing this value with the theoretical one of 240 MHz related to the measured lifetime through the relation $R_\infty \simeq (1/\tau_f)$ and assuming unitary quantum yield, we estimate a total collection efficiency of our setup at RT to be around 1%, ascribed to the limited numerical aperture of the optics and their transmission combined with the molecule emission profile.³⁴

In order to determine the alignment of DBT molecules within the Ac NCs, the emission from single molecules is detected by imaging the objective back focal plane (BFP) from which the angular radiation pattern can be deduced.⁵⁹ A typical BFP image is shown in the inset of Figure 2e, where the emission pattern features two side lobes facing each other beyond the critical angle, corresponding to the coupling between the evanescent wave in air with the propagative wave in the coverglass. The geometry and the direction of the two lobes confirms a horizontally aligned molecule, compatible with the XRD observations.

To conclude on the observed photophysical properties of the DBT:Ac NCs at RT, let us note that the repeated excitation of the same molecule to study its saturation behavior is a qualitative proof of the stability of its fluorescence. After several hours of measurements at RT, though, some molecules start exhibiting fluorescence blinking behavior, typically before they stop to fluoresce completely. This so-called photobleaching is most probably due to chemical reactions of the dye molecule with ambient oxygen,⁶⁰ a process that is more likely to occur in conjunction with the sublimation of Ac at RT. For sub-micrometric crystals we observe that sublimation at RT takes place on a time-scale of about one day but it is completely suppressed when covering the sample with a thin layer of a water-soluble polymer, such as poly(vinyl alcohol).

At cryogenic temperatures, highly doped DBT:Ac NCs are studied under resonant ex-

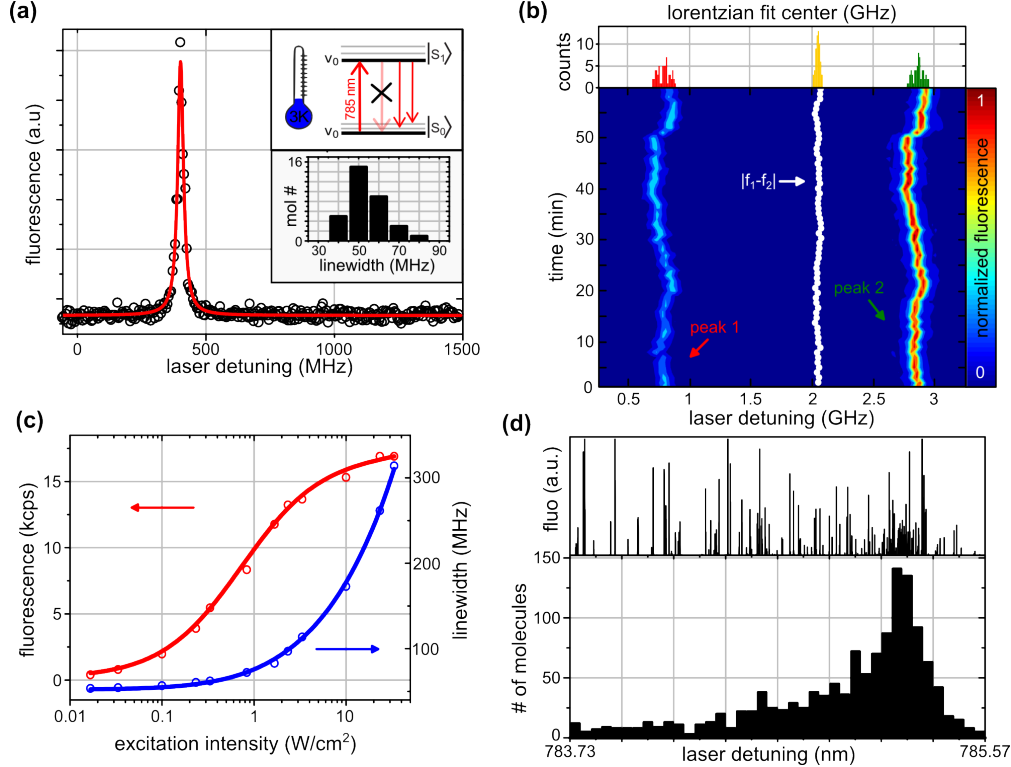


Figure 3: **Photophysics of the NCs at 2.9 K:** (a) Resonant excitation spectrum of a single DBT molecule in an Ac NC. The pumping scheme is sketched in the top-inset. Data (black circles) are fitted with a Lorentzian profile (red curve) and an average over four consecutive measurements yields a FWHM = (51 ± 10) MHz. The bottom-inset shows the linewidth distribution of 35 molecules. (b) 2D plot of the excitation spectrum in time, in a frequency range where two molecules within the same NC are excited. The difference of the two peak central frequencies is plotted as white circles in the map, while the relative distributions are shown as histograms in the top panel. (c) Saturation curve (red circles) and power broadening (blue circles) of the ZPL are displayed with the theoretical fits (solid lines), yielding a maximum number of detected photons $R_{\infty} = (16.8 \pm 0.4)$ kcps. (d)-**top** Excitation spectrum collected from a single NC within a frequency range of 800 GHz around 784.6 nm. (d)-**bottom** Inhomogeneous distribution of the ZPLs collected from 20 NCs.

citation of the so-called 00-Zero Phonon Line (ZPL) ($|S_{0,\nu_0}\rangle \rightarrow |S_{1,\nu_0}\rangle$). In this pumping scheme, sketched as an inset of Figure 3a, single DBT molecules can be addressed spectrally one at a time by tuning the frequency of a narrow-band laser and exploiting the inhomogeneous distribution of the molecular resonances. In fact, depending on the host matrix, the ZPLs of PAH molecules can be distributed over a frequency range that can be smaller than 1 GHz in unstressed sublimated crystals and as high as 10 THz in polymers or amorphous materials.^{61–63} We found that a DBT concentration about six orders of magnitude higher

than the one proposed for RT characterization allows to spectrally select single molecules within our experimental full range of about 800 GHz around 784.6 nm. This will be discussed further on in the manuscript.

Figure 3a shows the excitation spectrum of a single DBT molecule illuminated in confocal mode at 0.3 W cm^{-2} (below saturation), recording the red-shifted fluorescence as a function of the laser frequency (black circles). The spectral line is fitted with a Lorentzian profile (red curve) yielding a FWHM of 51 MHz, with an uncertainty of 10 MHz given by the standard deviation of four consecutive measurements of the same spectrum. Repeating this procedure on 35 molecules in different NCs leads to the distribution displayed in the inset of Figure 3a, with a low-width cutoff consistent with the lifetime-limited value of 40 MHz. The presence of molecules with broader linewidth can be explained in terms of the reduced size of the NC, which provides a less homogeneous environment for DBT molecules than that of bulk Ac. Moreover, interface effects on fluorescence stability and linewidth broadening are more likely to occur. However, let us note that the observed linewidth distribution is narrower than that measured by Gmeiner *et al.*,⁶⁴ confirming the high crystallinity of the Ac NC grown via reprecipitation.

Spectral diffusion has so far hindered the deployment of traditional (inorganic) NCs for narrow-band applications, such as single-photon sources for quantum technologies. We hence carefully analyze the spectral stability of the molecule transition frequency. In Figure 3b, the NC fluorescence counts detected from a SPAD are displayed in a 2D color map, obtained repeatedly scanning for 1 hour the excitation frequency of the pump laser over 10 GHz. The excitation of two different molecules can be recognized. The mean values and standard deviations for the two molecule ZPL frequencies over all measurements are (65 ± 6) MHz for peak 1 and (59 ± 4) MHz for peak 2. However, the common-mode fluctuation of the peak central frequencies is a clear indication of the non-negligible contribution given by the pump laser instability (the laser diode is thermally stabilized but not referred to any absolute frequency standard). To get rid of this contribution and highlight possible spectral

diffusion we analyze the distribution of the the two peak central frequencies difference (see the top panel in Figure 3b), plotted as white circles in the map. The maximum variation of such differential value is 17 MHz, which is well within the molecule linewidth and suggests negligible spectral diffusion for DBT:Ac NCs at 3 K. The same analysis has been carried out on couples of molecules in 8 different NCs. We observed sizable fluctuations only in one case where the ZPL central frequency over time exhibited a standard deviation of 54 MHz. As a term for comparison, we remind here that aromatic molecules in polymers or other amorphous hosts present linewidths as large as few GHz, accompanied by large spectral jumps (of the order of tens of GHz).^{63,65,66} Also, when molecules are embedded in a poor crystalline environment, a broadening of both linewidth and inhomogeneous distributions is observed, and spectral jumps, even if in a narrow frequency range of tens of MHz, are more likely to occur.⁶⁴

Figure 3c shows in logarithmic scale a typical saturation profile of a single molecule and its line broadening at low temperatures, obtained by measuring the excitation spectrum for several pump powers and plotting the detected count rates at resonance (blue circles) and the FWHMs (red circles) as a function of the excitation intensity. Detected counts are fitted with equation 1, providing a saturation intensity $I_s = (0.73 \pm 0.03) \text{ W cm}^{-2}$ and a maximum number of detected photons $R_\infty = (16.8 \pm 0.4) \text{ kcps}$ (free fitting parameters with the relative standard errors), or equivalently $R_\infty = 33.6 \text{ kcps}$ accounting for the detection efficiency η_{det} . This count rate is compatible with the collection efficiency of our experimental setup for low temperature measurements of about 0.3×10^{-3} , mainly due to the the orientation of the emissive dipole and the low numerical aperture of the collecting optics. The power broadening of the homogeneous spectral line $\gamma_{hom}(I)$ fits perfectly with the expected saturation law (blue line in Figure 3c) given by the equation:⁶⁷

$$\gamma_{hom}(I) = \gamma_{hom}(0) \left(1 + \frac{I}{I_s} \right)^{1/2} \quad (2)$$

which assumes negligible spectral diffusion, as previously demonstrated.

The inhomogeneous broadening of DBT molecules in Ac NCs is studied tuning the excitation laser over the available frequency range of about 800 GHz. In the top of Figure 3d a typical excitation spectrum collected at 2.9 K from a single NC is displayed, where we can distinguish about 80 peaks, each corresponding to a single molecule. The same measurement performed simultaneously on 20 NCs illuminated in wide-field for two orthogonal polarization of the laser pump allows to estimate the inhomogeneous distribution of the ZPLs of DBT molecules in Ac NCs. The result of this analysis is plotted in the histogram on the bottom of Figure 3d. We deduce a mean value of the transition frequency equal to 785.1 nm with a standard deviation of 0.4 nm, which is in agreement with the inhomogeneous broadening measured for other dyes in crystalline systems.⁵⁸ Finally, we observe that DBT:Ac NCs are ideal for the deterministic integration into nanophotonic devices, opening new perspectives on the use of molecules in the development of real-world quantum technologies.

Conclusions

In this work we demonstrate organic nanocrystals doped with quantum emitters, performing as efficient, photostable and scalable single-photon sources, at both room and cryogenic temperatures. In particular DBT:Ac crystals are presented, with an average size of few-hundreds nanometer. The growth procedure is based on reprecipitation, an inexpensive method that is adapted for a precise tuning of DBT concentration. Atomic force microscopy shows that the crystals grown under our experimental conditions present an average thickness of about 60 nm and an average size of 100 nm. The reported values can be controlled and reduced by varying the reprecipitation conditions, such as water temperature, droplet size, injected solution concentration and addition of surfactants. X-ray diffraction confirms the crystallinity of the nanoparticles and their platelet-like morphology. At room temperature, single DBT molecules in NCs show a maximum detected count rate of 1.5 MHz, a multi-photon prob-

ability lower than 5% and a well defined dipole orientation. At 2.9 K, the vast majority of molecules exhibits linewidths close to the lifetime-limited value and a relative narrow inhomogeneous distribution of 180 GHz around 785 nm. Accurate investigation on their photostability demonstrates that each NC embeds several molecules with stable fluorescence lines, with no signs of blinking or spectral diffusion on time scales of hours. These results may be extended to different molecular host-guest systems, functionalization protocols and purposes, making active organic nanocrystals a new toolbox for the integration of quantum emitters in photonic and optoelectronic circuits, as well as in complex hybrid devices.

Experimental Section

DBT:Ac NCs growth protocol. The DBT:Ac NCs growth procedure consists in injecting 250 μ L of a mixture 1 : 10⁶ of 1mM DBT-toluene and 5mM Ac-acetone solutions into 5 mL water. While continuously sonicating the system for 30 min, solvents dissolved in water and DBT:Ac crystals are formed in aqueous suspension. Solvents and Ac are purchased from Sigma Aldrich, water is deionized by a Milli-Q Advantage A10 System (18.2 m Ω cm at 25 °C) and DBT is purchased from Mercachem.

Morphological characterization. Crystals size is evaluated by scanning electron microscopy (SEM, Phenom Pro, PhenomWorld) and atomic force microscopy (AFM, Pico SPM from Molecular Imaging in AC mode equipped with a silicon probe NSG01 (NT-MDT) with 210 kHz resonant frequency). XRD measurements were performed at CRIST, the Crystallographic Centre of the University of Florence (Italy), with a XRD Bruker New D8 on a sample made of few μ L of suspension desiccated on a silicon-low background sample holder (Bruker AXS).

Optical setup. The optical characterization of DBT molecules within the sub-um Ac crystalline matrix was performed with a versatile home-built scanning fluorescence confocal microscope. The setup is equipped with a closed cycle Helium cryostat (Cryostation

by Montana Instruments), capable of cooling samples down to 2.9 K. Molecules can be excited at 767 nm either by a continuous wave laser (CW, Toptica DL110-DFB) and a pulsed Ti:Sapphire (200 fs pulse width, 81.2 MHz repetition rate) laser. Alternatively, at cryogenic temperature, resonant excitation is performed with a narrowband fiber-coupled CW laser (Toptica, LD-0785-0080-DFB-1) centered at 784.6 nm, whose frequency can be scanned continuously over a range of 800 GHz. All laser sources are linearly polarized to allow optimal coupling to single DBT transition by means of a half-wave plate in the excitation path. The laser intensities reported in the main text are calculated from the power measured at the objective entrance divided by the area of the confocal spot measured on the bare substrate (in both cases larger than the diffraction limited spot). For low temperature measurements, the excitation light is focused onto the sample by a long working distance air objective (Mitutoyo 100 \times Plan Apochromat, NA = 0.7, WD = 6 mm) and can be scanned over the sample through a telecentric system and a dual axis galvo-mirror. For room temperature measurements, a high-NA oil immersion objective (Zeiss Plan Apochromat, 100 \times , NA= 1.4) is used to focus light on the sample which is mounted on a piezoelectric nanopositioner (NanoCube by Physik Instrumente). The Stokes-shifted fluorescence is collected by the same microscope objective used in excitation, separated from the excitation light through a dichroic mirror (Semrock FF776-Di01) and a longpass filter (Semrock RazorEdge 785RS-25) and detected by either an EM-CCD camera (Andor iXon 885, 1004 \times 1002 pixels, pixel size 8 μm \times 8 μm) or two single-photon avalanche diodes (τ -SPAD-50 Single Photon Counting Modules by PicoQuant). SPADs can be used independently or in a Hanbury Brown-Twiss (HBT) configuration, using a time-correlated single-photon counting (TCSPC) card (PicoHarp, PicoQuant). A converging lens can be inserted in the excitation path to switch between confocal and wide-field illumination while a converging lens is added in the detection path before the EMCCD camera to study the wave-vector distribution of the light emitted by single DBT molecules via BFP imaging.

Notes

The authors declare no competing financial interest.

Acknowledgement

The authors would like to thank S. Ciattini, L. Chelazzi (CRIST) for helping with XRD measurements, M. Mamusa for dynamic light scattering experiments, F. Intonti for the microinfiltration setup, D. S. Wiersma for access to clean room facilities, M. Bellini and C. Corsi for Ti:sapphire operation, K.G. Schädler and F.H.L. Koppens for helpful feedback on the NCs properties and useful discussions about integration in hybrid devices. This work benefited from the COST Action MP1403 (Nanoscale Quantum Optics). The authors acknowledge financial support from the Fondazione Cassa di Risparmio di Firenze (GRANCASSA) and MIUR program Q-Sec Ground Space Communications.

References

- (1) Kovalenko, M. V. et al. Prospects of Nanoscience with Nanocrystals. ACS Nano **2015**, 9, 1012–1057.
- (2) Zheng, X. T.; Ananthanarayanan, A.; Luo, K. Q.; Chen, P. Glowing graphene quantum dots and carbon dots: properties, syntheses, and biological applications. Small **2015**, 11, 1620–1636.
- (3) Lyu, Y.; Xie, C.; Chechetka, S. A.; Miyako, E.; Pu, K. Semiconducting polymer nanobioconjugates for targeted photothermal activation of neurons. Journal of the American Chemical Society **2016**, 138, 9049–9052.
- (4) Kim, T.-H.; Jun, S.; Cho, K.-S.; Choi, B. L.; Jang, E. Bright and stable quantum dots and their applications in full-color displays. MRS Bulletin **2013**, 38, 712–720.

- (5) Talapin, D. V.; Lee, J.-S.; Kovalenko, M. V.; Shevchenko, E. V. Prospects of Colloidal Nanocrystals for Electronic and Optoelectronic Applications. Chemical Reviews **2010**, 110, 389–458.
- (6) O’Brien, J. L.; Furusawa, A.; Vučković, J. Photonic quantum technologies. Nature Photonics **2009**, 3, 687–695.
- (7) Aharonovich, I.; Englund, D.; Toth, M. Solid-state single-photon emitters. Nature Photonics **2016**, 10, 631–641.
- (8) Gatto Monticone, D.; Katamadze, K.; Traina, P.; Moreva, E.; Forneris, J.; Ruo-Berchera, I.; Olivero, P.; Degiovanni, I. P.; Brida, G.; Genovese, M. Beating the Abbe Diffraction Limit in Confocal Microscopy via Nonclassical Photon Statistics. Phys. Rev. Lett. **2014**, 113, 143602.
- (9) Sangouard, N.; Zbinden, H. What are single photons good for? Journal of Modern Optics **2012**, 59, 1458–1464.
- (10) Tillmann, M.; Tan, S.-H.; Stoeckl, S. E.; Sanders, B. C.; de Guise, H.; Heilmann, R.; Nolte, S.; Szameit, A.; Walther, P. Generalized Multiphoton Quantum Interference. Phys. Rev. X **2015**, 5, 041015.
- (11) Knill, E.; Laflamme, R.; Milburn, G. J. A scheme for efficient quantum computation with linear optics. nature **2001**, 409, 46–52.
- (12) QuantumManifesto, available at <http://quope.eu/manifesto>, **2016**.
- (13) Lounis, B.; Orrit, M. Single-photon sources. Reports On Progress In Physics **2005**, 68, 1129–1179.
- (14) Chu, X.-L.; Götzinger, S.; Sandoghdar, V. A single molecule as a high-fidelity photon gun for producing intensity-squeezed light. Nat Photon **2017**, 11, 58–62.

- (15) Loredo, J. C.; Broome, M. A.; Hilaire, P.; Gazzano, O.; Sagnes, I.; Lemaitre, A.; Almeida, M. P.; Senellart, P.; White, A. G. Boson Sampling with Single-Photon Fock States from a Bright Solid-State Source. Physical Review Letters **2017**, 118, 130503.
- (16) Sipahigil, A.; Jahnke, K. D.; Rogers, L. J.; Teraji, T.; Isoya, J.; Zibrov, A. S.; Jelezko, F.; Lukin, M. D. Indistinguishable photons from separated silicon-vacancy centers in diamond. Physical Review Letters **2014**, 113, 113602.
- (17) Lettow, R.; Rezus, Y. L. A.; Renn, A.; Zumofen, G.; Ikonen, E.; Göttinger, S.; Sandoghdar, V. Quantum Interference of Tunably Indistinguishable Photons from Remote Organic Molecules. Phys. Rev. Lett. **2010**, 104, 123605.
- (18) Bermudez-Urena, E.; Gonzalez-Ballesteros, C.; Geiselmann, M.; Marty, R.; Radko, I. P.; Holmgaard, T.; Alaverdyan, Y.; Moreno, E.; Garcia-Vidal, F. J.; Bozhevolnyi, S. I.; Quidant, R. Coupling of individual quantum emitters to channel plasmons. Nat Commun **2015**, 6.
- (19) Schroeder, T.; Schell, A. W.; Kewes, G.; Aichele, T.; Benson, O. Fiber-Integrated Diamond-Based Single Photon Source. Nano Lett. **2011**, 11, 198–202.
- (20) Liebermeister, L.; Petersen, F.; Münchow, A. v.; Burchardt, D.; Hermelbracht, J.; Tashima, T.; Schell, A. W.; Benson, O.; Meinhardt, T.; Krueger, A.; Stiebeiner, A.; Rauschenbeutel, A.; Weinfurter, H.; Weber, M. Tapered fiber coupling of single photons emitted by a deterministically positioned single nitrogen vacancy center. Applied Physics Letters **2014**, 104, 031101.
- (21) Riedrich-Möller, J.; Arend, C.; Pauly, C.; Mücklich, F.; Fischer, M.; Gsell, S.; Schreck, M.; Becher, C. Deterministic Coupling of a Single Silicon-Vacancy Color Center to a Photonic Crystal Cavity in Diamond. Nano Letters **2014**, 14, 5281–5287.
- (22) Schell, A. W.; Kaschke, J.; Fischer, J.; Henze, R.; Wolters, J.; Wegener, M.; Benson, O.

- Three-dimensional quantum photonic elements based on single nitrogen vacancy-centres in laser-written microstructures. Scientific reports **2013**, 3.
- (23) Shi, Q.; Sontheimer, B.; Nikolay, N.; Schell, A. W.; Fischer, J.; Naber, A.; Benson, O.; Wegener, M. Wiring up pre-characterized single-photon emitters by laser lithography. Scientific Reports **2016**, 6, 31135.
- (24) Somaschi, N.; Giesz, V.; De Santis, L.; Loredano, J.; Almeida, M. P.; Hornecker, G.; Portalupi, S. L.; Grange, T.; Antón, C.; Demory, J. Near-optimal single-photon sources in the solid state. Nature Photonics **2016**, 10, 340–345.
- (25) Sapienza, L.; Davanço, M.; Badolato, A.; Srinivasan, K. Nanoscale optical positioning of single quantum dots for bright and pure single-photon emission. Nature Communications **2015**, 6, 7833.
- (26) Arcari, M.; Söllner, I.; Javadi, A.; Lindskov Hansen, S.; Mahmoodian, S.; Liu, J.; Thyrrstrup, H.; Lee, E.; Song, J.; Stobbe, S.; Lodahl, P. Near-Unity Coupling Efficiency of a Quantum Emitter to a Photonic Crystal Waveguide. Physical Review Letters **2014**, 113, 093603.
- (27) Daveau, R. S.; Balram, K. C.; Pregolato, T.; Liu, J.; Lee, E. H.; Song, J. D.; Verma, V.; Mirin, R.; Nam, S. W.; Midolo, L.; Stobbe, S.; Srinivasan, K.; Lodahl, P. Efficient fiber-coupled single-photon source based on quantum dots in a photonic-crystal waveguide. Optica **2017**, 4, 178–184.
- (28) Zadeh, I. E.; Elshaari, A. W.; Jöns, K. D.; Fognini, A.; Dalacu, D.; Poole, P. J.; Reimer, M. E.; Zwiller, V. Deterministic Integration of Single Photon Sources in Silicon Based Photonic Circuits. Nano Letters **2016**, 16, 2289–2294.
- (29) Davanço, M.; Liu, J.; Sapienza, L.; Zhang, C.-Z.; De Miranda Cardoso, J. V. c.; Verma, V.; Mirin, R.; Nam, S. W.; Liu, L.; Srinivasan, K. Heterogeneous integra-

- tion for on-chip quantum photonic circuits with single quantum dot devices. Nature Communications **2017**, 8, 889.
- (30) Hausmann, B. J. M.; Shields, B.; Quan, Q.; Maletinsky, P.; McCutcheon, M.; Choy, J. T.; Babinec, T. M.; Kubanek, A.; Yacoby, A.; Lukin, M. D.; Lončar, M. Integrated Diamond Networks for Quantum Nanophotonics. Nano Letters **2012**, 12, 1578–1582.
- (31) Mouradian, S. L.; Schröder, T.; Poitras, C. B.; Li, L.; Goldstein, J.; Chen, E. H.; Walsh, M.; Cardenas, J.; Markham, M. L.; Twitchen, D. J.; Lipson, M.; Englund, D. Scalable Integration of Long-Lived Quantum Memories into a Photonic Circuit. Phys. Rev. X **2015**, 5, 031009.
- (32) Türschmann, P.; Rotenberg, N.; Renger, J.; Harder, I.; Lohse, O.; Utikal, T.; Göttinger, S.; Sandoghdar, V. Chip-Based All-Optical Control of Single Molecules Coherently Coupled to a Nanoguide. Nano Letters **2017**, 17, 4941–4945.
- (33) Lombardi, P.; Ovvyan, A.; Pazzagli, S.; Mazzamuto, G.; Kewes, G.; Neitzke, O.; Gruhler, N.; Benson, O.; Pernice, W.; Cataliotti, F. Photostable molecules on chip: integrated single photon sources for quantum technologies. ACS Photonics **2017**,
- (34) Checcucci, S.; Lombardi, P.; Rizvi, S.; Sgrignuoli, F.; Gruhler, N.; Dieleman, F. B.; Cataliotti, F. S.; Pernice, W. H.; Agio, M.; Toninelli, C. Beaming light from a quantum emitter with a planar optical antenna. Light: Science & Applications **2016**, 6, e16245.
- (35) Skoff, S. M.; Papencordt, D.; Schauffert, H.; Bayer, B. C.; Rauschenbeutel, A. An optical nanofiber-based interface for single molecules. arXiv preprint arXiv:1604.04259 **2016**,
- (36) Pisanello, F.; Leménager, G.; Martiradonna, L.; Carbone, L.; Vezzoli, S.; Desfonds, P.; Cozzoli, P. D.; Hermier, J.-P.; Giacobino, E.; Cingolani, R.; De Vittorio, M.; Bra-

- mati, A. Non-Blinking Single-Photon Generation with Anisotropic Colloidal Nanocrystals: Towards Room-Temperature, Efficient, Colloidal Quantum Sources. Adv. Mater. **2013**, 25, 1974–1980.
- (37) Liu, J.; Konthasinghe, K.; Davanço, M.; Lawall, J.; Anant, V.; Verma, V.; Mirin, R.; Nam, S. W.; Song, J. D.; Ma, B. Direct observation of nanofabrication influence on the optical properties of single self-assembled InAs/GaAs quantum dots. arXiv preprint arXiv:1710.09667 **2017**,
- (38) Empedocles, S. A.; Bawendi, M. G. Quantum-confined stark effect in single CdSe nanocrystallite quantum dots. Science **1997**, 278, 2114–2117.
- (39) Efros, A. L.; Nesbitt, D. J. Origin and control of blinking in quantum dots. Nat Nano **2016**, 11, 661–671.
- (40) Chandrasekaran, V.; Tessier, M. D.; Dupont, D.; Geiregat, P.; Hens, Z.; Brainis, E. Nearly Blinking-Free, High-Purity Single-Photon Emission by Colloidal InP/ZnSe Quantum Dots. Nano Lett. **2017**, –.
- (41) Park, Y.-S.; Guo, S.; Makarov, N. S.; Klimov, V. I. Room Temperature Single-Photon Emission from Individual Perovskite Quantum Dots. ACS Nano **2015**, 9, 10386–10393.
- (42) Raino, G.; Nedelcu, G.; Protesescu, L.; Bodnarchuk, M. I.; Kovalenko, M. V.; Mahrt, R. F.; Stöferle, T. Single Cesium Lead Halide Perovskite Nanocrystals at Low Temperature: Fast Single-Photon Emission, Reduced Blinking, and Exciton Fine Structure. ACS Nano **2016**, 10, 2485–2490.
- (43) Jantzen, U.; Kurz, A. B.; Rudnicki, D. S.; Schäfermeier, C.; Jahnke, K. D.; Andersen, U. L.; Davydov, V. A.; Agafonov, V. N.; Kubanek, A.; Rogers, L. J.; Jelezko, F. Nanodiamonds carrying silicon-vacancy quantum emitters with almost lifetime-limited linewidths. New Journal of Physics **2016**, 18, 073036.

- (44) Tran, T. T.; Kianinia, M.; Bray, K.; Kim, S.; Xu, Z.-Q.; Gentle, A.; Sontheimer, B.; Bradac, C.; Aharanovich, I. Nanodiamonds with photostable, sub-gigahertz linewidths quantum emitters. arXiv preprint arXiv:1705.06810 **2017**,
- (45) Toninelli, C.; Early, K.; Breimi, J.; Renn, A.; Sandoghdar, V. Near-infrared single-photons from aligned molecules in ultrathin crystalline films at room temperature. Optics Express **2010**, 18, 6577–6582.
- (46) Nicolet, A. A.; Hofmann, C.; Kol’chenko, M. A.; Kozankiewicz, B.; Orrit, M. Single dibenzoterrylene molecules in an anthracene crystal: Spectroscopy and photophysics. ChemPhysChem **2007**, 8, 1215–1220.
- (47) Trebbia, J.-B.; Ruf, H.; Tamarat, P.; Lounis, B. Efficient generation of near infra-red single photons from the zero-phonon line of a single molecule. Optics Express **2009**, 17, 23986–23991.
- (48) Horn, D.; Rieger, J. Organic nanoparticles in the aqueous phase - Theory, experiment, and use. Angewandte Chemie International Edition **2001**, 40, 4330–4361.
- (49) Kasai, H.; Nalwa, H. S.; Oikawa, H.; Okada, S.; Matsuda, H.; Minami, N.; Kakuta, A.; Ono, K.; Mukoh, A.; Nakanishi, H. A novel preparation method of organic microcrystals. Japanese Journal of Applied Physics **1992**, 31, L1132.
- (50) Kang, P.; Chen, C.; Hao, L.; Zhu, C.; Hu, Y.; Chen, Z. A novel sonication route to prepare anthracene nanoparticles. Materials Research Bulletin **2004**, 39, 545–551.
- (51) Baba, K.; Kasai, H.; Nishida, K.; Nakanishi, H. Nanocrystal; InTech, 2011.
- (52) Chung, H.-R.; Kwon, E.; Oikawa, H.; Kasai, H.; Nakanishi, H. Effect of solvent on organic nanocrystal growth using the reprecipitation method. Journal of crystal growth **2006**, 294, 459–463.

- (53) Brock, C. P.; Dunitz, J. Temperature dependence of thermal motion in crystalline anthracene. Acta Crystallographica Section B: Structural Science **1990**, 46, 795–806.
- (54) Nicolet, A. A.; Hofmann, C.; Kol’chenko, M. A.; Kozankiewicz, B.; Orrit, M. Single dibenzoterrylene molecules in an anthracene crystal: Main insertion sites. ChemPhysChem **2007**, 8, 1929–1936.
- (55) Meltzer, R.; Yen, W.; Zheng, H.; Feofilov, S.; Dejneka, M.; Tissue, B.; Yuan, H. Evidence for long-range interactions between rare-earth impurity ions in nanocrystals embedded in amorphous matrices with the two-level systems of the matrix. Physical Review B **2001**, 64, 100201.
- (56) Mazzamuto, G.; Tabani, A.; Pazzagli, S.; Rizvi, S.; Reserbat-Plantey, A.; Schädler, K.; Navickaite, G.; Gaudreau, L.; Cataliotti, F.; Koppens, F. Single-molecule study for a graphene-based nano-position sensor. New Journal of Physics **2014**, 16, 113007.
- (57) Polisseni, C.; Major, K. D.; Boissier, S.; Grandi, S.; Clark, A. S.; Hinds, E. Stable, single-photon emitter in a thin organic crystal for application to quantum-photonics devices. Optics Express **2016**, 24, 5615–5627.
- (58) Moerner, W. E.; Fromm, D. P. Methods of single-molecule fluorescence spectroscopy and microscopy. Review of Scientific Instruments **2003**, 74, 3597–3619.
- (59) Lieb, M. A.; Zavislan, J. M.; Novotny, L. Single-molecule orientations determined by direct emission pattern imaging. JOSA B **2004**, 21, 1210–1215.
- (60) Kozankiewicz, B.; Orrit, M. Single-molecule photophysics, from cryogenic to ambient conditions. Chem. Soc. Rev. **2014**, 43, 1029–1043.
- (61) Veerman, J.; Garcia-Parajo, M.; Kuipers, L.; Van Hulst, N. Single molecule mapping of the optical field distribution of probes for near-field microscopy. Journal of Microscopy **1999**, 194, 477–482.

- (62) Kramer, A.; Segura, J.-M.; Hunkeler, A.; Renn, A.; Hecht, B. A cryogenic scanning near-field optical microscope with shear-force gapwidth control. Review of scientific instruments **2002**, 73, 2937–2941.
- (63) Kozankiewicz, B.; Bernard, J.; Orrit, M. Single molecule lines and spectral hole burning of terrylene in different matrices. The Journal of chemical physics **1994**, 101, 9377–9383.
- (64) Gmeiner, B.; Maser, A.; Utikal, T.; Götzinger, S.; Sandoghdar, V. Spectroscopy and microscopy of single molecules in nanoscopic channels: spectral behavior vs. confinement depth. Physical Chemistry Chemical Physics **2016**, 18, 19588–19594.
- (65) Walser, A.; Zumofen, G.; Renn, A.; Götzinger, S.; Sandoghdar, V. Spectral dynamics and spatial localization of single molecules in a polymer. Molecular Physics **2009**, 107, 1897–1909.
- (66) Boiron, A.-M.; Tamarat, P.; Lounis, B.; Brown, R.; Orrit, M. Are the spectral trails of single molecules consistent with the standard two-level system model of glasses at low temperatures? Chemical physics **1999**, 247, 119–132.
- (67) Ambrose, W.; Basché, T.; Moerner, W. Detection and spectroscopy of single pentacene molecules in ap-terphenyl crystal by means of fluorescence excitation. The Journal of Chemical Physics **1991**, 95, 7150–7163.

Graphical TOC Entry

